Dyes and Pigments 84 (2009) 128–133

Contents lists available at ScienceDirect

Dyes and Pigments

journal homepage: www.elsevier.com/locate/dyepig

Dielectric relaxation dynamics in liquid crystal – dye composites

Muklesur Rahman [a], Chien-Wen Hsieh [a], Chun-Tsai Wang [a], Bo-Ru Jian [a], Wei Lee [b,*]

[a] Department of Physics, Chung Yuan Christian University, Chung-Li 32023, Taiwan
[b] Department of Physics and Center for Nanotechnology, Chung Yuan Christian University, Chung-Li 32023, Taiwan

ARTICLE INFO

Article history:
Received 6 February 2009
Received in revised form
11 July 2009
Accepted 13 July 2009
Available online 21 July 2009

Keywords:
Liquid crystals
Dyes
C.I. acid red 2
C.I. Disperse blue 14
Dielectric spectroscopy
Dielectric relaxation

ABSTRACT

Dielectric relaxation spectroscopic studies were undertaken to investigate the role of the resistivity of a host liquid crystal in the relaxation dynamics of dyed systems. Two different types of liquid crystal mixture were used, namely, one that was characterized by high ion contamination and low resistivity and the other which was of high resistivity and virtual ion-free; both types were doped using an azo or anthraquinone dye. Dielectric spectra of both the pristine liquid crystals and their composites at different external fields were measured in homogenously-aligned cells. The use of both dyes on an ion-enriched liquid crystal not only enhanced ion concentration but also slowed down the relaxation process. In contrast, the relaxation process for composites with a high-resistivity liquid crystal host was faster than that of the pristine liquid crystal.

1. Introduction

Calamitic (rod-like) nematic liquid crystals (NLCs) are well known for their widespread application in liquid crystal display (LCD) devices. Owing to their large optical anisotropy (i.e., birefringence) and dielectric anisotropy, NLCs have also been used to modulate refractive index by molecular reorientation with an external field or under the action of light [1]. Nowadays, to obtain materials with eutectic physical properties for displays or other optical devices, different additives such as carbon nanotubes [2–4], metal nanoparticles [5–7] and dyes [8–10] are doped in pure liquid-crystalline materials. Two main classes of aromatic dyes have enjoyed use as guests in LC mixtures as azo dyes have been employed as dopants in condensed optical materials intended for novel opto-electronic devices. Recently, nonlinear effects of azo dye-doped liquid crystals (ADDLCs), such as photorefractive-like effects [11,12] and degenerate four-wave mixing [13], have attracted much attention. Moreover, an extraordinarily high Kerr coefficient has been detected in a mixture of low-molar-mass NLC (5CB) and the azo dye C.I. Acid Red 2 [Methyl Red (MR) [14]]; this combination had attracted attention in the context of holographic gratings [15,16] including intensity gratings [17]. It has been demonstrated that a small amount of dye (~1%) dissolved in NLC enhances the reorientation of the NLC molecules by almost two orders of magnitude [18,19]. As a consequence of such enhanced reorientation, changes in the relaxation dynamics of LC–dye composite systems from that of the pristine NLC occurs. Because the dielectric tensor changes with applied field as a result of director reorientation, dielectric relaxation in NLCs is intrinsically more complex than that in isotropic fluids and solid crystals and, hence, the dynamics of complex LC systems presents more challenges. Dielectric relaxation is determined by a number of processes, some of which (electronic polarizability, intra-molecular vibrations) are very fast, with a characteristic duration of <1 ns, while others, such as reorientation of the permanent molecular dipoles, are slow, with a typical relaxation time τ of ~0.01–1 ms. Studies of dielectric as well as impedance spectra have been carried out to investigate the effects of azo and anthraquinone dyes on the dielectric parameters of a NLC [20–22]. In these studies, the relaxation frequencies of ADDLC (E7 + MR) have been found to shift to the lower frequencies (slow relaxation) irrespective of biased or unbiased conditions. However, the relaxation mechanisms of these composite systems are much more complicated from those of the pure LC materials and depend upon the molecular structure of the host as well as that of the dopant. Further rigorous relaxation studies on the different LC systems doped with different types of dyes could reveal the relaxation dynamics clearly.

To investigate the effect of dyes on the relaxation dynamics of an NLC, two types of LC mixtures and two dissimilar dyes were selected; the LC materials were chosen on the basis of ion-richness and bulk resistivity. Dielectric relaxation spectra, using different

* Corresponding author. Tel.: +886 3 265 3228; fax: +886 3 265 3299.
E-mail address: wlee@cycu.edu.tw (W. Lee).

0143-7208/$ – see front matter © 2009 Elsevier Ltd. All rights reserved.
doi:10.1016/j.dyepig.2009.07.005

bias fields, were measured and relaxation parameters calculated using the Debye model.

2. Experimental

2.1. Materials

Two NLC systems with distinctive levels of impurity-ion concentration were used, namely, the well-known, low-resistivity nematic E7 and an ultrapure TFT-grade nematic mixture designated as CYLC-01. The host material, E7, developed in the 1970s, exhibits a stable nematic phase over the range of −10 °C to +60 °C [23]; it is a eutectic mixture of four cyano compounds (4′-*n*-pentyl-4-cyanobiphenyl (5CB), 4′-*n*-heptyl-4-cyanobiphenyl (7CB), 4′-*n*-octyloxy-4-cyanobiphenyl (8OCB) and 4″-*n*-pentyl-4-cyano-*p*-triphenyl (5CT) [24]). Due to its high polarity, E7 displays a strong permanent dipole moment along the molecular axis, possesses large dielectric anisotropy ($\Delta\varepsilon \sim 14$ at 1 kHz and 20 °C [23]) and is notorious for its vulnerability to contamination with ionic impurities. As cyano compounds are known to have low resistivity and possess high concentration of ionic impurities, the nematic E7, of bulk resistivity ρ of $10^9\,\Omega\,m$ [23], is not employed in the TFT–LCD industry. In contrast, CYLC-01 developed in the 2000s, with nematic-to-isotropic transition temperature T_{NI} at 80.1 °C, is a CF_2O-based, superfluorinated LC mixture used in the current active-matrix LCD market. This TFT-grade LC material has $\Delta\varepsilon = 4.6$ at 1 kHz and 20 °C and very high ρ of $4.6 \times 10^{12}\,\Omega\,m$ at 25 °C. In general, superfluorinated LC mixtures such as CYLC-01, molecularly designed for modern LCD technology, are known to have high resistivity and low ion concentration in the expense of dielectric anisotropy. E7 was purchased from Merck and CYLC-01, customerized by Merck, was obtained from a local manufacturer of TFT–LCD panels. Both of the mesogenic substances have been used without any further modification.

The dichroic dyes used were the azo dye C.I. Acid Red 2 (Methyl Red, MR), 2-[4-(dimethylamino)phenylazo]benzoic acid, and the anthraquininoid dye C.I. Disperse Blue 14 (DB14), 1,4-bis(methylamino)anthraquinone (Fig. 1) [25]. The dyes were obtained from Aldrich, USA and Lancaster, England, respectively. While no information on the purity of MR can be found, the purity of DB14 was 95%.

2.2. Sample preparation

The LCs were doped with C.I. Acid Red 2 and C.I. Disperse Blue 14 of 1% by weight at room temperature. The uniformly dispersed suspensions were prepared by mixing an LC and a dye using a minishaker followed by ultrasonic agitation in a bath. The solubility of both dyes in the TFT-grade LC host CYLC-01 was noticeably lower than that in the cyano nematic host E7, presumably due to the different degree of polarity. Owing to the limited amount of either additive, T_{NI} of the solutions were found to be indifferent (within experimental uncertainty) from the measured transition for the pristine LC.

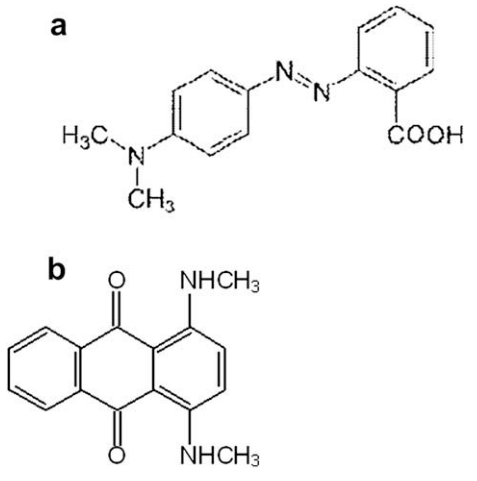

Fig. 1. Molecular structures of the two dyes, (a) Acid Red 2 and (b) Disperse Blue 14, used in the present study.

To fabricate a standard LC cell, the inner surfaces of two glass substrates were first coated with transparent and electrically conductive indium–tin-oxide (ITO) layers. A thin polyimide film was layered onto each conducting substrate and rubbed unidirectionally to promote a strong planar alignment. Empty cells were then filled by capillary action in the isotropic phase of the respective dye-doped systems and allowed to slowly cool down to room temperature to favor the LC alignment. The alignment layer induced a small pretilt angle ($\sim 2^\circ$) of the nematic director (i.e., the average direction of the long molecular axes of NLC molecules) from the substrate plane. Cells consisting of neat NLCs were also fabricated as a reference. Totally, six types (E7, E7–C.I. Acid Red 2, E7–C.I. Disperse Blue 14, CYLC-01, CYLC-01–C.I. Acid Red 2, CYLC-01–C.I. Disperse Blue 14) of cells were made in terms of the material confined in cells. All cells were examined under an optical polarizing microscope prior to adoption for an experiment. Shielded parallel-plate capacitors used in the experiments were of area of $1 \times 1\,cm^2$ and thickness of $4.4 \pm 0.1\,\mu m$ as determined by interference.

2.3. Measurements

In a typical dielectric experiment, one monitors the frequency dependence of the complex dielectric constant governed by the molecular polarizability and structural arrangement. The complex dielectric constant is conventionally expressed by $\varepsilon^* = \varepsilon' - i\varepsilon''$ [26], where i denotes the imaginary unit and the dielectric dispersion ε' and the dielectric loss (also termed dielectric absorption) ε'' are the real and imaginary parts of the frequency-dependent dielectric constant, respectively. We carried out dielectric measurements with a computer-controlled Agilent E4980A precision LCR meter having a bias voltage range ±40 V and frequency range from 20 Hz to 2 MHz. Sinusoidal signal of 500-mV amplitude was used to measure simultaneously the values of capacitance and conductance, with a time interval of 2 s between two successive measurements. Using these conductance and capacitance values, dielectric losses and dielectric dispersions have been calculated. All of the dielectric spectra were acquired in sandwich-type planar cells at the same temperature (25.0 °C) and other identical conditions. In order to ensure the reliability of the data, at least eight samples of each type of cells were investigated and averaged data were obtained from measurements on the same type of samples.

3. Results and discussion

An ITO-coated empty cell itself exhibits the so-called "cell relaxation" due to the RC circuit formed by the resistance and capacitance of the parallel-plate electrodes in series with the tin–ITO contact resistance. Such cell relaxation frequencies are usually observed in the MHz frequency range and almost independent of temperature [27,28]. The empty cells used in our investigation also showed a cell relaxation with relaxation frequency near 1.8 MHz.

LC systems exhibit dielectric anisotropy due to their structural anisotropy. The dielectric anisotropy, referring to the difference in dielectric dispersion, is written as $\Delta\varepsilon \equiv \varepsilon_{\parallel} - \varepsilon_{\perp}$, where $\varepsilon_{\parallel}$ and $\varepsilon_{\perp}$ are the parallel and perpendicular components of the real dielectric constant. The director is predetermined by the interfacial

alignment layers and can be reoriented by the application of an electric field beyond the Fréedericksz transition [29]. As such, the tilt angle of the LC director and, in turn, the effective dielectric constant vary with the applied voltage. For an NLC with positive dielectric anisotropy (i.e., $\Delta\varepsilon > 0$), ideally planar-configured molecules being perpendicular to the measuring field exhibit the smallest dielectric dispersion $\varepsilon' = \varepsilon_{\perp}$. As the applied voltage increases across the cell thickness, the angle between the nematic director and the field decreases until the LC becomes homeotropically (or vertically) aligned and the dielectric dispersion reaches its largest value $\varepsilon' = \varepsilon_{\parallel}$.

Fig. 2(a) and (b) illustrates the dielectric spectra of pure and composite systems based on the host materials E7 and CYLC-01, respectively. For simplicity, C.I. Acid Red 2 and C.I. Disperse Blue 14 are designated MR and DB14, respectively, in the legends of the figures. The experimental relaxation spectra were fitted with the Debye equation [30] for the real and imaginary parts of the complex dielectric constant

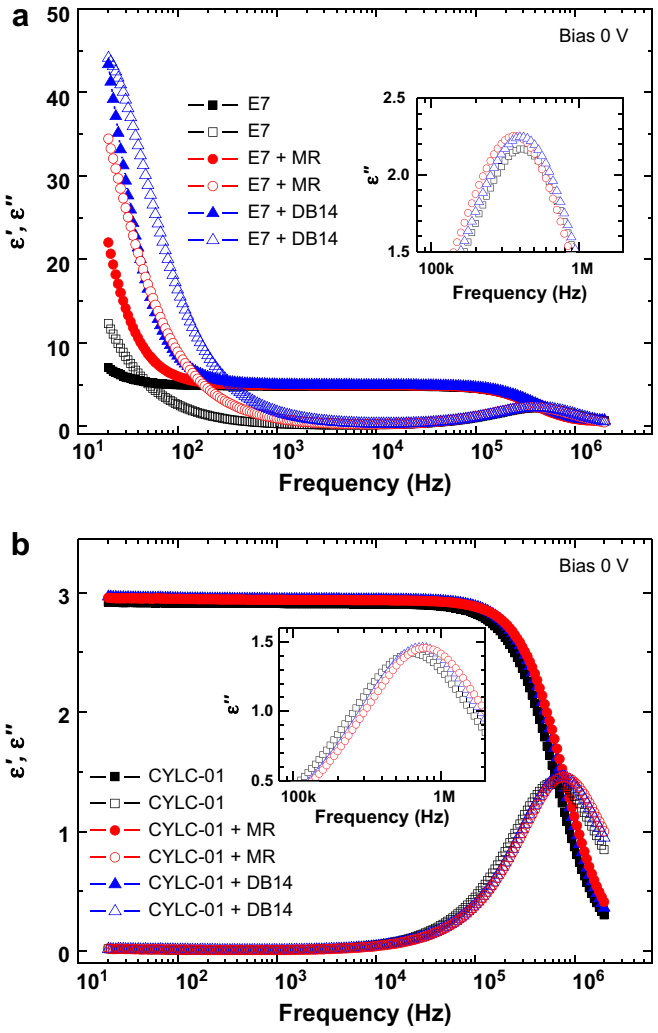

Fig. 2. Dielectric relaxation spectra of (a) an ion-enriched LC mixture (E7) and its composites with azo and anthraquinone dyes and (b) a TFT-grade LC mixture (CYLC-01) and its composites. The solid and open symbols correspond to the real and imaginary parts of the relaxation, respectively. The inset in (a) depicts a zooming view of the relaxation regime of E7 systems. The solid lines are the fitted curves based on Eq. (1b). The experimental spectra of E7 and its composites differ significantly at lower frequencies from the theoretical formulation. Such deviation is due to the contribution from ion charges and fitted well with Eq. (2) (dotted lines). Lending of dyes in E7 enhances the ion density into the composites.

$$\varepsilon' = \varepsilon_{\infty} + \frac{\varepsilon_s - \varepsilon_{\infty}}{1 + \omega^2\tau^2} \tag{1a}$$

and

$$\varepsilon'' = \frac{(\varepsilon_s - \varepsilon_{\infty})\omega\tau}{1 + \omega^2\tau^2} \tag{1b}$$

where the symbols ε_s and ε_{∞} stand for the dielectric constants in the static (or low-frequency) and high-frequency limits, respectively, and ω and τ represent the angular frequency and the relaxation time, respectively. The relaxation time corresponds to the critical or dielectric relaxation frequency f_c, where the dielectric loss reaches a maximum and the dielectric anisotropy changes the sign from positive to negative. The dielectric relaxation frequencies have been determined by these fitting parameters.

The dielectric relaxation spectra of all these six materials at a fixed temperature (25.0 °C) in nematic phase exhibit only one prominent relaxation peak at a relaxation time of the order of 10^{-6} s. However, few weak relaxation processes have been reported earlier in the nematic phase of LC mixtures [31]. The relaxation time suggests that the relaxation process is associated with the rotational motion of the molecules along the short axis. The relaxation time tied in relation with rotational motion along the long axis is much shorter than the observed relaxation time. Moreover, to be ensured that the relaxation mode is solely due the rotational motion of the molecules and not to cell relaxation, we performed experiments with LC cells of different thicknesses (≥4.5 μm) and found the position of the relaxation frequency to remain almost unchanged. Comparing the dielectric spectra of the two pristine LCs, it is ensured that the dielectric spectrum of ion-enriched LC E7 (Fig. 2(a)) only shows an unusual increment in dielectric loss values at lower frequencies. Again the relaxation peak of E7 is relatively broader than that for the other materials. The theoretical Cole–Cole equation for relaxation fitted well (continuous lines in Fig. 2) in the whole frequency range (20 Hz to 2 MHz) with the experimental spectra of CYLC-01, whereas for E7 the spectra at lower frequencies deviate significantly from the theoretical formulation. Such deviations at lower frequencies are attributed to the ion charges present in the pristine thermotropic polar LC mixture E7, however, it should be mentioned that there are always some ion charges being generated by the manufacturing process of the experimental cells or devices. We have used similar kind of LC cells for all the experiments. These ion charges contribute mostly at the low frequencies to the dielectric loss value, which is expressed by [32]

$$\varepsilon'' = \frac{\delta_0}{\varepsilon_0\omega^{1-s}} \tag{2}$$

where ε_0 is the free-space permittivity and δ_0 is the fitting parameter representing the electrical conductivity. The power-law exponent s is generally less than one, indicating a polaron-hoping-type conduction mechanism. Eq. (2) fitted well (dotted line in Fig. 2(a)) with the low-frequency relaxation spectra of E7 with $\delta_0 = 1.8918 \times 10^{-7}$ (ohm m)$^{-1}$ and $s = 0.04341$. Interestingly, when such an ion-enriched LC mixture was used as the host for the LC–dye composite system, the values of ε'' at lower frequencies have been found to be larger than that for the pristine one, as shown in

Table 1
Dielectric relaxation frequencies of pristine LCs and their composites in absence of a bias.

LC material	f_c (Hz)		
	LC	LC–MR	LC–DB14
E7	510 281.3	345 396.7	419 820.7
CYLC-01	632 455.5	751 674.8	766 918.5

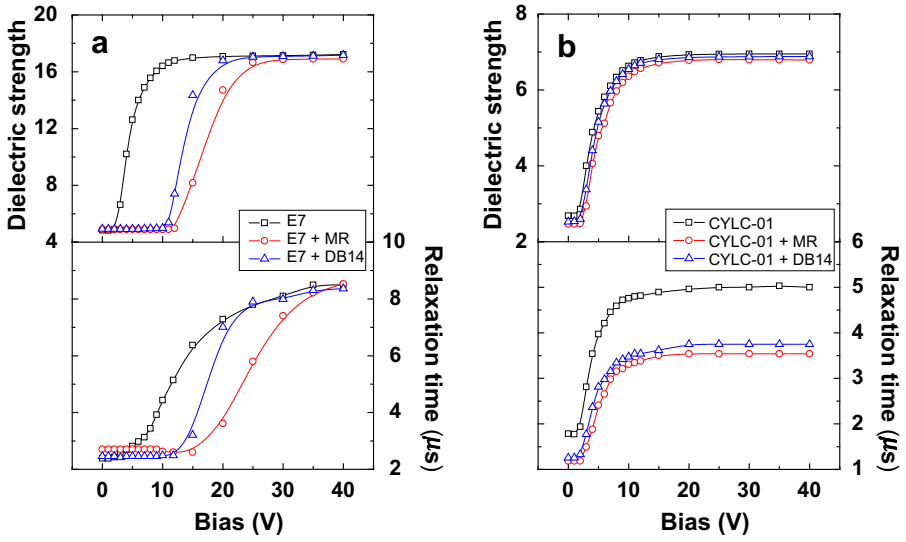

Fig. 3. Variation of dielectric strength and relaxation time with applied bias voltage for (a) E7 and (b) CYLC-01, with their composites. The relaxation times for the composites of CYLC-01 are shorter than that for pristine CYLC-01, but the relaxation process of dyed composites of E7 slows down. The threshold voltage for composites of E7 also increases due to enhancement in ion concentration, whereas the threshold voltages for composites of CYLC-01 remain almost same.

Fig. 2(a). The values of δ_0, calculated by using Eq. (2), are 3.9139×10^{-7} (ohm m)$^{-1}$ and 4.3165×10^{-7} (ohm m)$^{-1}$ for E7–Acid Red 2 and E7–Disperse Blue 14, respectively, suggesting enhancement of the ion charges into the composites. The values of δ_0 imply that the anthraquinone disperse dye C.I. Disperse Blue 14 generates more ion charges in comparison with C.I. Acid Red 2 for the same low-resistivity host material. The polar nature of the E7 molecules and the dyes is responsible for such enhancement of ion concentration in the composite systems. However, for the composite systems with high-resistivity LC material (CYLC-01) as host, no significant changes have been observed into the values of low-frequency dielectric loses.

The relaxation frequencies of the composite systems also exhibit significant changes but with different manners depending on the host LC material. The relaxation frequencies of the pure and their composite systems are listed in Table 1. It is clear that the composites of E7 exhibit significantly decreased relaxation frequencies compared with that of their neat counterpart. On the contrary, the relaxation frequencies of the composites with CYLC-01 as the host material are larger than that of its pure form. From the experimental results it is concluded that the relaxation process speeds up and slows down for the LC–dye composite systems with high-resistivity LC and ion-rich LC, respectively, as host.

External bias voltage changes the orientational direction of the nematic director under the interaction between applied field and the dielectric anisotropy of the LC. The external bias forces the director to align in the direction of the applied field and the degree of rotation depends on the magnitude of the applied field. Sufficient external field is needed to overcome the viscous as well as the anchoring forces. Here it is interesting to note that the solid dopants like carbon nanotube also align themselves along with the director [33]. On the other hand, it is still not clear how the molecules of the organic dyes behave under the external field. Using Eq. (2) and experimental dielectric spectra, we have determined the dielectric relaxation time (frequency) and dielectric strength $(\varepsilon_s - \varepsilon_\infty)$ as a function of external bias for pure LCs and their composites. Fig. 3(a) and (b) shows the dielectric strength and relaxation time varying with bias voltage for LC materials E7 and CYLC-01, respectively, along with their composites. Fig. 3 clearly shows that at lower voltages both the dielectric strength and relaxation time do not change, but after a threshold voltage (V_{th}) both increase nonlinearly and reach at saturation after a higher

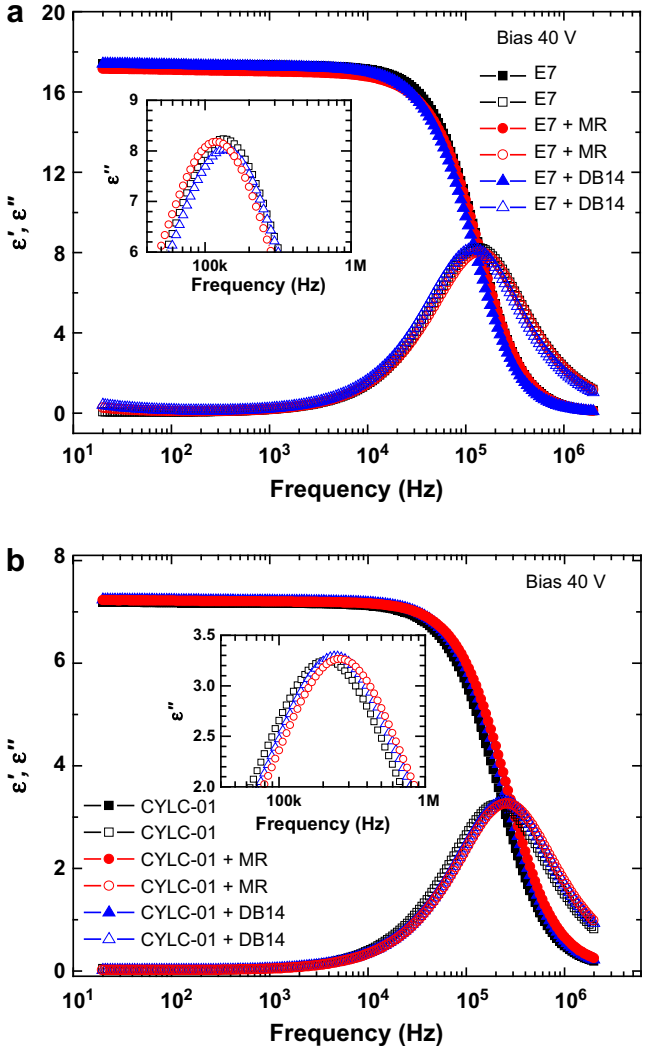

Fig. 4. Dielectric relaxation spectra at external bias of 40.0 V of (a) an ion-enriched NLC (E7) and its composites containing Acid Red 2 and Disperse Blue 14 dyes and (b) a high-resistivity NLC (CYLC-01) and its composites. Inset in (a), expanded scale in the regime of dielectric relaxation. The solid and open symbols are associated with the real and imaginary parts of the relaxation, respectively.

critical field. However, little differences have been observed into the values of the threshold voltages for dielectric strength and relaxation frequency. Fig. 3(a) clearly shows that V_{th} for the composites E7–C.I. Acid Red 2 and E7–C.I. Disperse Blue 14 are larger than that for the pure E7. This is clearly a consequence of the growth of ion charges into the composite systems. These ions are often adsorbed on the interfaces between the polyimide alignment and LC layers, generating a directionally anticipating internal barrier. The width of the internal barrier increases with increasing the density of ions and hence more electric bias is needed to overcome the barrier. The threshold voltages for the composites (Fig. 3(b)) constructed by the LC material CYLC-01 do not show any significant changes from those of the pristine material. Such results are in good agreement with the dielectric spectra which do not show any significant changes in the ion densities inside the composites. Hence one can conclude that the high-resistivity LC material is much more suitable than the ion-enriched and low-resistivity materials for LC–dye composite systems.

At sufficiently high external bias voltage the nematic director of LC molecules align themselves along with the applied field. In such homeotropic state the relaxation time increases considerably. Although this relaxation process is linked with the rotation of the LC molecules along the short axis (as in planar cell) but the relaxation process becomes slower due to the dielectric memory effect

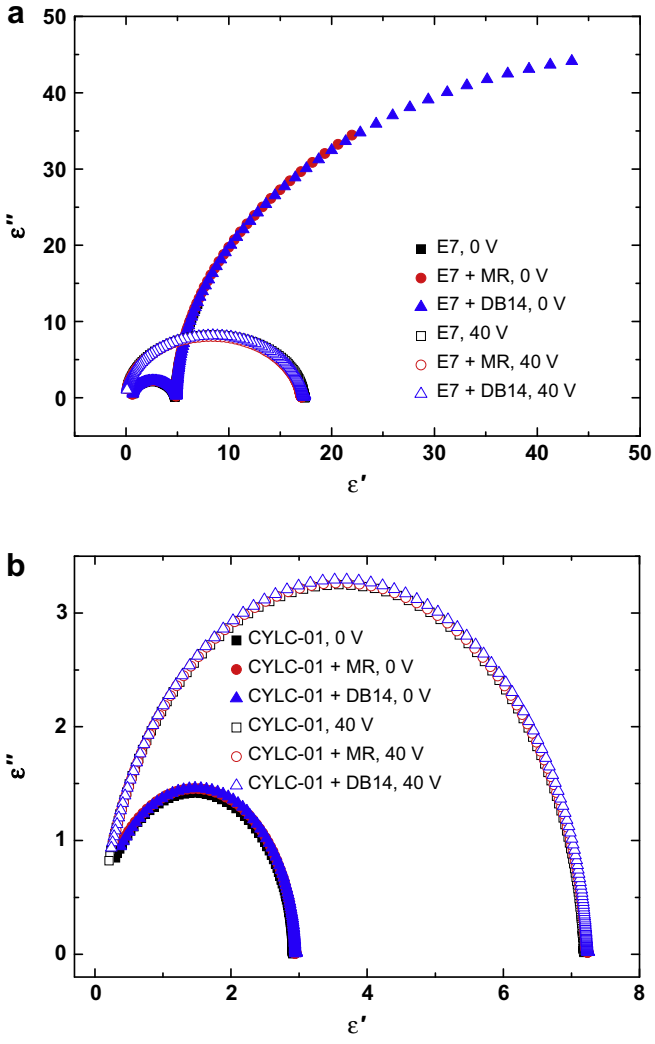

Fig. 5. Cole–Cole plots in unbiased (0 V) and biased (40 V) conditions for (a) E7 and (b) CYLC-01 with their dyed composites.

Table 2
Dielectric relaxation frequencies of pristine LCs and their composites with 40.0 V bias voltage.

LC material	f_c (Hz)		
	LC	LC–MR	LC–DB14
E7	130 193.5	129 631.2	114 182.1
CYLC-01	215 097.5	246 713.0	240 038.3

(DME) in presence of electric field [34].Fig. 4(a) and (b) illustrates the dielectric (storage and loss) spectra of pure and composite systems with host materials E7 and CYLC-01, respectively, with a 40.0-V bias voltage. In the condition with a dc bias, the relaxation times of the composite systems constructed with E7 are larger than that for the pristine host. But again for the TFT-grade LC host the composite systems relax faster than their pure host. In Fig. 5 we show the corresponding Cole–Cole plots in the planar and homeotropic states, at null voltage and 40 V, respectively, for both E7 and CYLC-01 as well as their composites. Table 2 shows the values of the relaxation frequencies of the hosts and the composite systems. In view of Table 1 as well as Table 2, it is disclosed that the relaxation process of the composites fabricated with the high-resistivity host is faster than the host's pristine form in all director geometry.

4. Conclusions

In conclusion, effects of the physical properties of the LC on the relaxation process of LC–dye composite systems have been studied by dielectric relaxation spectroscopy. It has been unambiguously shown that the relaxation process of NLC–dye composites manufactured with an ion-enriched as well as low-resistivity LC slows down in comparison with the pristine materials. We believe that this regularity established in this work is true not only for E7 but also for other ion-rich LC materials in that E7 is a typical representative of its class. On the other hand, the dielectric relaxation time decreases for the composites made up with high-resistivity LCs such as the TFT-grade mesogenic substance CYLC-01 employed in this study. In this case, the result may change depending on the polarity as well as polarizability of the LC molecules. Further investigations involving other fields of spectroscopy, such as NMR and Raman spectroscopy, would be more useful to demonstrate this phenomenon.

Acknowledgements

The authors are thankful to Ssu-Hao Liao and Feng-Cheng Hsu for help in preparing mixtures of dye-doped CYLC-01 and taking dielectric spectra for Figs. 2(b) and 4(b). This work was supported by the National Science Council of the Republic of China (Taiwan) under Grant No. NSC 95-2112-M-033-012-MY3.

References

[1] Khoo I-C. Liquid crystals. 2nd ed. Hoboken, New Jersey: Wiley; 2007.
[2] Lee W, Wang C-Y, Shih Y-C. Effects of carbon nanosolids on the electro-optical properties of a twisted nematic liquid-crystal host. Applied Physics Letters 2004;85:513.
[3] Baik I-S, Jeon SY, Lee SH, Park KA, Jeong SH, An KH, et al. Electrical-field effect on carbon nanotubes in a twisted nematic liquid crystal cell. Applied Physics Letters 2005;87:263110.
[4] Chen H-Y, Lee W. Suppression of field screening in nematic liquid crystals by carbon nanotubes. Applied Physics Letters 2006;88:222105.
[5] Thisayukta J, Shiraki H, Sakai Y, Masumi T, Kundu S, Shiraishi Y, et al. Dielectric properties of frequency modulation twisted nematic LCDs doped with silver nanoparticles. Japanese Journal of Applied Physics 2004;43:5430.
[6] Qi H, Kinkead B, Hegmann T. Effects of functionalized metal and semiconductor nanoparticles in nematic liquid crystal phases. Proceedings of Society of Photo-Optical Instrumentation Engineers 2008;6911:691106.

[7] Paoloni S, Mercuri F, Marinelli M, Zammit U, Neamtu C, Dadarlat D. Simultaneous characterization of optical and thermal parameters of liquid-crystal nanocolloids with high-temperature resolution. Physical Review E 2008;78:042701.
[8] Piccardi A, Assanto G, Lucchetti L, Simoni F. All-optical steering of soliton waveguides in dye-doped liquid crystals. Applied Physics Letters 2008;93:171104.
[9] Fedorenko D, Slyusarenko K, Ouskova E, Reshetnyak V, Ha KR, Karapinar R, et al. Light-induced gliding of the easy orientation axis of a dye-doped nematic liquid crystal. Physical Review E 2008;77:061705.
[10] Simpson SH, Richardson RM, Hanna S. Influence of dye molecules on the birefringence of liquid crystal mixtures at near infrared frequencies. Journal of Chemical Physics 2007;127:104901.
[11] Khoo IC. Orientational photorefractive effects in nematic liquid crystal films. IEEE Journal of Quantum Electronics 1996;32:525.
[12] Lee M-R, Wang J-R, Lee C-R, Fuh AY-G. Optically switchable biphotonic photorefractive effect in dye-doped liquid crystal films. Applied Physics Letters 2004;85:5822.
[13] Tomov IV, Dutton TE, VanWonterghem B, Rentzepis PM. Temperature dependence of degenerate four wave mixing in azo dye doped polymer films. Journal of Applied Physics 1991;70:36.
[14] Khoo IC, Slussarenko S, Guenther BD, Shih M-Y, Chen P, Wood WV. Optically induced space-charge fields, dc voltage, and extraordinarily large nonlinearity in dye-doped nematic liquid crystals. Optics Letters 1998;23(4):253.
[15] Khoo IC, Li H, Liang Y. Optically induced extraordinarily large negative orientational nonlinearity in dye-doped liquid crystal. IEEE Journal of Quantum Electronics 1993;29(5):1444.
[16] Fuh AY-G, Lee C-R, Cheng K-T. Fast optical recording of polarization holographic grating based on an azo-dye-doped polymer-ball-type polymer-dispersed liquid crystal film. Japanese Journal of Applied Physics 2003;42:4406.
[17] Fuh AY-G, Liao C-C, Hsu K-C, Lu C-L. Laser-induced reorientation effect and ripple structure in dye-doped liquid-crystal films. Optics Letters 2003;28:1179.
[18] Janossy I, Lloyd AD. Low-power optical reorientation in dyed nematics. Molecular Crystals and Liquid Crystals 1991;203:77.
[19] Janossy I. Molecular interpretation of the absorption-induced optical reorientation of nematic liquid crystals. Physical Review E 1994;49:2957.
[20] Özder S, Okutan M, Köysal O, Göktas H, San SE. Effect of an azo dye (DR1) on the dielectric parameters of a nematic liquid crystal system. Physica B 2007;390:101.
[21] Okutan M, Yakuphanoglu F, San SE, Köysal O. Impedance spectroscopy and dielectric anisotropy-type analysis in dye-doped nematic liquid crystals having different preliminary orientations. Physica B 2005;368:308.
[22] Dunmur DA. The determination of molecular parameters from dielectric measurements on nematic liquid crystals. Liquid Crystals 2005;32:1379.
[23] Merck data sheets.
[24] Lee W, Shih Y-C. Effects of carbon-nanotube doping on the performance of a TN-LCD. Journal of the Society for Information Display 2005;13(9):743.
[25] Okutan M, San SE, Köysal O. Dielectric spectroscopy analysis of molecular reorientation in dye doped nematic liquid crystals having different preliminary orientation. Dyes and Pigments 2005;65:169.
[26] Jonscher AK. Dielectric relaxation in solids. London: Chelsea Dielectrics Press; 1983.
[27] Cava RJ, Patel JS, Reitman EA. Audio frequency dielectric response of the liquid-crystal CE8 in chiral and racemic forms. Journal of Applied Physics 1986;60:3093.
[28] Cava R, Patel JS, Collen KR, Goodby JW, Rietman EA. Thin-cell dielectric response of a ferroelectric liquid crystal. Physical Review A 1987;35:4378.
[29] Rahman M, Lee W. Scientific duo of carbon nanotubes and nematic liquid crystals. Journal of Physics D: Applied Physics 2009;42:063001.
[30] Cole KS, Cole RH. Dispersion and absorption in dielectrics I. Alternating current characteristics. Journal of Chemical Physics 1941;9:341.
[31] Viciosa MT, Nunes AM, Fernandes A, Almedia PL, Godinho MH, Dionisio MD. Dielectric studies of the nematic mixture E7 on a hydroxypropylcellulose substrate. Liquid Crystals 2002;29:429.
[32] Mott NF, Davis EA. Electronic processes in non-crystalline materials. Oxford: Oxford University Press; 1979.
[33] Dierking I, Scalia G, Morales P, LeClere D. Aligning and reorienting carbon nanotubes with nematic liquid crystals. Advanced Materials 2004;16:865.
[34] Gu M, Yin Y, Shiyanovskii SV, Lavrentovich OD. Effects of dielectric relaxation on the director dynamics of uniaxial nematic liquid crystals. Physical Review E 2007;76:061702.